ANNALS OF FACULTY ENGINEERING HUNEDOARA
- INTERNATIONAL JOURNAL OF ENGINEERING
Tome IX (Year 2011). Fascicule 3. (ISSN 1584 - 2673)

[1.] Mohamed A. A. EL-SHAER

NONLINEAR ANALYSIS OF CIRCULAR COMPOSITE COLUMNS

[1.] CIVIL & CONSTRUCTION ENGINEERING DEPARTMENT, HIGHER TECHNOLOGICAL INSTITUTE, 10TH OF RAMADAN CITY, CAIRO, EGYPT

ABSTRACT: The finite element is introduced to describe the behavior of circular columns: confined, partially confined or reinforced with fiber reinforced polymers (FRP). Geometric and material nonlinearities are taken into consideration. The column is analyzed under axial force together with a biaxial moment applied at its ends. This paper presents the initial results of a study aimed at quantifying the increase in strength of columns due to introducing FRP in different methods. Results show that using FRP as external wrapping gives higher increase in strength than using it as embedded reinforcement.
KEYWORDS: finite element method, circular columns, fiber reinforced polymers (FRP)

❖ INTRODUCTION

Reinforcing or confining concrete columns with FRP have received significant attention for use in civil infrastructures due to their unique properties, such as the high strength to weight ratio and stiffness-to-weight ratio, corrosion and fatigue resistance and tailorability. Most of research works in field focus on axially loaded columns. Rousakis, Karabinis, Kiousis, and Tepfers (2008) used a strain-hardening Drucker-Prager model for the assessment and calibration of the elasto-plastic behavior of FRP confined concrete. Issa and Alrousan (2009) presented an experimental and nonlinear finite element analysis to determine the strength and ductility of circular short concrete columns confined externally with carbon fiber-reinforced polymer subjected to pure axial loading. Harajli (2006) developed a general mathematical model to describe the stress-strain relationship for FRP confined concrete. Lam and Teng (2009) modeled the stress strain behavior of FRP-confined concrete under cyclic compression. Other researchers focused on retrofitting short columns. Binici (2008) conducted a parametric study on a typical bridge column for different axial loads, reinforcement ratios and FRP amounts. Harajli (2009) conducted an experimental program and deduced design expression evaluating the minimum thickness of FRP jacket required for seismic steel-concrete bond strengthening. Tastani and Pantazopoulou (2008) used a database of published experiments on R.C. beam columns tested under cyclic loading after being jacketed by FRPs to assess rules for the problem. Cheng, Solelino and Chen (2004) studied the effects of design parameters on the ultimate strength of a circular column confined by FRP. Tavarez, Bank and Plesha (2003) used a finite element analysis to predict the behavior of concrete beams with FRP embedded in the concrete as reinforcement.

The ultimate strength that defines the combinations of axial load and biaxial end moment of concrete short and slender columns with FRP is of great interest in the present analysis. Interaction diagrams are proposed to provide a practical method for engineers to evaluate the ultimate strength of the column under consideration.

❖ STRESS-STRAIN RELATIONSHIPS OF MATERIALS – STRESS STRAIN RELATIONSHIP FOR CONCRETE

The stress-strain models of confined and unconfined concrete proposed by Saadatmansh and Ehsani (1974) and based on the work of several other researchers, Popovics (1973) and Scott, Park and Priestly (1982) will be summarized herein and adopted for the analysis of concrete columns externally reinforced with fiber composite straps. However, some relations were simplified by the writers. The stress-strain model shown in Figure1 is based on an equation proposed by Popovics (1973). The longitudinal compressive concrete stress f_c is defined as:

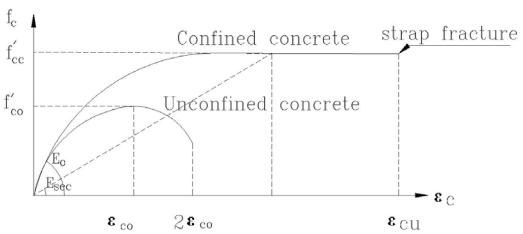

Figure 1. Stress-strain curve for concrete

$$f'_c = \frac{f'_{cc} x^r}{r - 1 + x^r} \quad (1)$$

where

$$x = \frac{\varepsilon_c}{\varepsilon_{cc}} \quad (2)$$

$$\varepsilon_{cc} = \varepsilon_{co}\left[1+\left[\frac{f'_{cc}}{f'_{co}}-1\right]\right] \quad (3)$$

$$r = \frac{E_c}{E_c - E_{sec}} \quad (4)$$

$$E_{sec} = \frac{f'_{cc}}{\varepsilon_{cc}} \quad (5)$$

$$f'_{cc} = f'_{co} + \left[\sqrt{\frac{f_{l/}}{f'_{co}}} * f'_{co}\left(1-\frac{s'}{s''}\right)\right] \quad (6)$$

where: s= the strap width, $s^{/}$= the uncovered width repeated along the column, s'' = the distance between the midpoints of the widths of two successive straps. s, s', s'' are shown in Figure 2, f'_{cc} = compressive strength of confined concrete, f'_{co} = unconfined concrete strength, ϵ_c=longitudinal compressive strain of concrete, ϵ_{cu}= strain at maximum concrete stress, ϵ_{co}= 0.002, is the strain at maximum concrete stress f'_{co} of unconfined concrete, E_c =tangent modulus of elasticity of concrete, E_{sec}= secant modulus of confined concrete at peak stress and $f_l^{/}$= effective lateral confining pressure from transverse reinforcement assumed to be uniformly distributed over the surface of the concrete core.

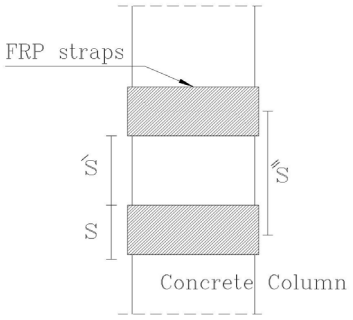

Figure 2. Longitudinal Section of the Column

Mander, Priestly and Park (1988) proposed an effective lateral confining pressure by transverse reinforcements on the concrete section. This effective pressure is defined as:

$$f_l' = f_l k_e \quad (7)$$

where

$$k_e = \frac{A_e}{A_{cc}} \quad (8)$$

where: f'_l= lateral pressure from transverse reinforcement; K_e= confinement effectiveness coefficient; A_e= area of effectively confined concrete core; and A_{cc}= effective area of concrete enclosed by composite strap given by

$$A_{cc} = A_c(1-\rho_{cc}) \quad (9)$$

where: $\rho_{cc=}$ ratio of area of longitudinal reinforcement to gross area of concrete and A_c= area of concrete enhanced by composite strap.

The confining pressure induced on the concrete core by the composite strap is calculated by considering the free body of the column cross section confined by the strap as shown in Figure 3.

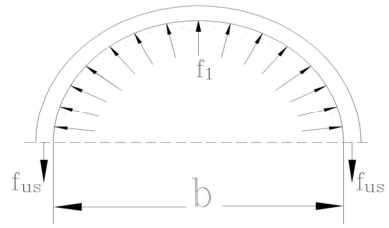

Figure 3. Confining Action of the Composite strap

The outward expansion of the concrete core is prevented by the action of the strap placed in horizontal tension. From equilibrium of forces the confining stress can be calculated as:

$$f_l = \frac{2f_{us}A_{st}}{bs} \quad (10)$$

where: f_{us}= ultimate strength of composite strap; A_{st}= cross-sectional area of strap and b= diameter of column.

The area of effectively confined concrete core midway between the levels of straps can be calculated from

$$A_e = \frac{\pi}{4}\left(b-\frac{s'}{2}\right)^2 = \frac{\pi b}{4}\left(1-\frac{s'^{\cdot}}{2b}\right)^2 \quad (11)$$

Substituting Eqs. (12 and 14) in Eq. (11) results in the confinement effectiveness coefficient for circular section given by

$$k_e = \frac{\left(1-\frac{s'^{\cdot}}{2b}\right)^2}{1-\rho_{cc}} \quad (12)$$

In Figure 1 for unconfined and confined concrete, the area under each stress-strain curve represents the total strain energy per unit volume of concrete at failure. The difference between these two areas is provided for by the confining effect of the composite strap. The ultimate compression strain of concrete at the point of fracture of the confining composite strap can be calculated, resulting in complete determination of the stress-strain curve of the confined concrete throughout the entire range of loading up to the fracture of composite strap and consequent strain of the column saadatmanesh, Ehsani and li (1994).

❖ STRESS STRAIN RELATIONSHIP FOR STRAPS

Composite straps behave linearly elastic to failure. Figure 4 shows the stress-strain relationship for carbon fiber composite straps used in this paper.

The modulus of elasticity of carbon straps is 1.65E7 t/m^2 and its normal strength is 2.80762E5 t/m^2.

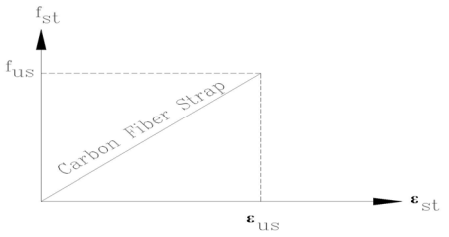

Figure 4. Stress-Strain Curves for Straps

❖ STRESS STRAIN RELATIONSHIP FOR STEEL

For simplicity, the stress-strain relationship for the steel bars is considered to be an elastic-perfectly plastic curve neglecting steel hardening. The relationship is shown in Figure 5 .The steel has a yield strength f_y of 4.06E4 t/m^2.

The Figure shows that f_s is the steel stress; f_y is the specified yield strength of steel; ε_s is the steel strain and ε_y is the steel yield strain.

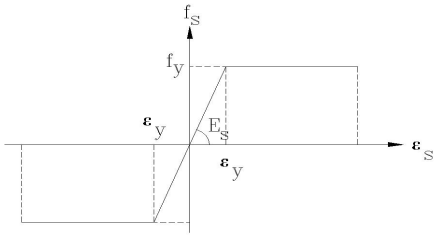

Figure 5. Stress-strain curve for steel

❖ METHOD OF SOLUTION BY PARTITIONING OF THE CROSS-SECTION

A force F_x is considered to act at eccentricities e_y and e_z as shown in Figure 6. A section discretization of the circular concrete column and FRP is applied and shown in Figure 7, hence all elemental areas are summed up to obtain the cross-section properties.

The maximum value of Z denoted by Z_{max} measured to the lower extreme fiber from the origin is

$$Z_{max} = Z_{min} + b \qquad (13)$$

ϵ_o , ϵ_u , ϵ_m are the strain at point o, strain at the imaginary point Q and the maximum strain at the extreme concrete fibers respectively.

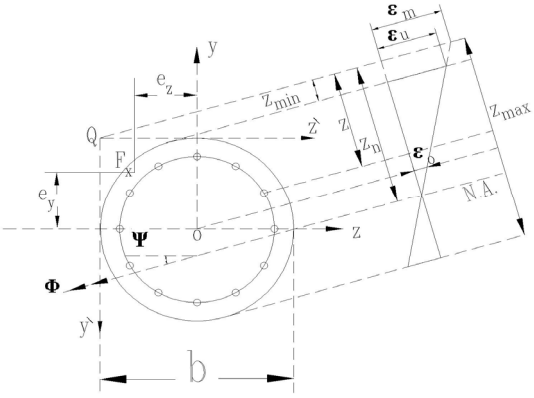

Figure 6. Force vector and strain distribution

The formulation of equations for the analysis of a circular column of concrete containing a circular array of longitudinal bars and a steel section of irregular dimensions is rather difficult. When a nonlinear stress distribution is imposed on this composite section, the analysis is further complicated. To overcome these difficulties a member cross section can be partitioned or subdivided into discrete elemental areas as shown in Figure 7.

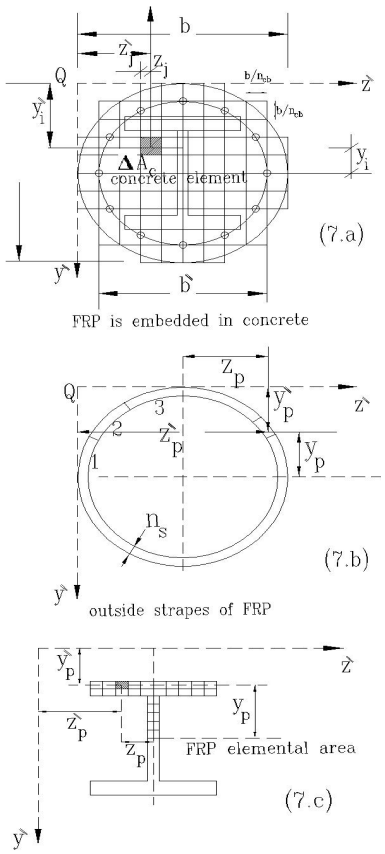

Figure 7. Partitioning of the cross-section

The y\ and z\ coordinates to the centroids of the concrete elemental areas measured from the origin Q shown in Figure 7a can be more readily evaluated by the computer when the partitioning grid mesh is regularly spaced. If the number of columns in a grid, n_{cb}, equals the number of rows, then each concrete element $\Delta A_c = (b/n_{cb})^2 = 4A_c/\Pi n^2_{cb}$.

By denoting the elemental concrete area at the i, jth position of the grid by ΔA_{cij} and the coordinates of its centroid by z'_j and y'_i, then $z'_j = (2j-1)b/2n_{cb}$ and $y'_i = (2i-1)b/2n_{cb}$. Knowing these coordinates, the distance to the center of gravity of the composite column section from each concrete element ΔA_{cij} can be calculated as $[(b/2-z'_j)^2+(b/2-y'_i)^2]^{1/2}$. If this distance is less than the radius of the circular concrete section, b/2, then ΔA_{cij} is effective, and if the distance is greater than or equal to b/2, then ΔA_{cij} is equated to zero or ignored.

The longitudinal bars are assumed evenly spaced around a circle of diameter b". If the total bar steel area=Asb, the total number of bars=nb, and if one steel elemental area, ΔAsb, equals one bar area, then ΔAsb= Asb/nb. Let the z\ and y\ coordinates of the centroids of the bar element ΔA_{sbk} at the k_{th} position, measured from the origin shown in Figure 7b be denoted by $z^{\backslash}_k$ and $y^{\backslash}_k$, then

$$z^{\backslash}_k = \frac{b-b''}{2} + \frac{b''}{2}\{1-\cos[(k-1)\frac{2\Pi}{n_b}]\} \qquad (14)$$

$$y^{\backslash}_k = \frac{b-b''}{2} + \frac{b''}{2}\{1-\sin[(k-1)\frac{2\Pi}{n_b}]\} \qquad (15)$$

And the ratio of a steel bar to an elemental concrete are ρ_k is expressed as

$$\rho_k=\Delta A_b/\ \Delta A_{cij} \tag{16}$$

In case of confining with FRP, the elemental area at position p is of coordinates $y'_p$and z'_p as given below:

$$y'_p=\frac{b}{2}\left[1-\sin\left((p-1)*\frac{2\Pi}{n_{st}}+\frac{\Pi}{n_{st}}\right)\right] \tag{17}$$

$$Z'_p=\frac{b}{2}\left[1-\cos\left((p-1)*\frac{2\Pi}{n_{st}}+\frac{\Pi}{n_{st}}\right)\right] \tag{18}$$

where n_{st} is the total number of elemental strap areas in one ring around the column.

Figure 7c shows the partitioning of the FRP plates into n_p elemental areas the centroidal coordinates from Q are y'_p and z'_p.

By denoting the elemental area of FRP at the p_{th} position by ΔA_p, then

$$\rho_p=\Delta A_p/\ \Delta A_{cij} \tag{19}$$

Since a linear strain distribution across the section is assumed, the strains at the centroids of each elemental area can be found using the stress-strain relationships. The corresponding stresses can be computed. Differentiating the stress-strain relationship for concrete, steel bars and FRP gives

$$\delta f_c = G_c\delta\varepsilon_c \tag{20}$$

$$\delta f_s = G_s\delta\varepsilon_s \tag{21}$$

$$\delta f_{st} = G_{st}\delta\varepsilon_{st} \tag{22}$$

where G_c. G_s and G_{st} are the elemental modulii of elasticity for concrete, steel and FRP respectively.

Consequently the properties of the cross section can be determined by summing up the properties of the elemental areas as shown below

$$EA=\left[\sum_{i=1}^{n_{cb}}\sum_{j=1}^{n_{cb}}(G_c)_{ij}+\rho_k\sum_{k=1}^{n_b}(G_s)_k+\rho_p\sum_{p=1}^{n_{st}}(G_{st})_p-\rho_p\sum_{p=1}^{n_{st}}(G_c)_p-\rho_k\sum_{k=1}^{n_b}(G_c)_k\right]\Delta A_c \tag{23}$$

$$EI_y=\left[\sum_{i=1}^{n_{cb}}\sum_{j=1}^{n_{cb}}(z_j)^2(G_c)_{ij}+\rho_k\sum_{k=1}^{n_b}(z_k)^2(G_s)_k-\rho_k\sum_{k=1}^{n_b}(z_k)^2(G_c)_k\right]\Delta A_c+\left[\rho_p\sum_{p=1}^{n_{st}}(Z_p)^2(G_{st})_p-\rho_p\sum_{p=1}^{n_{st}}(Z_p)^2(G_c)_p\right]\Delta A_c \tag{24}$$

$$EI_z=\left[\sum_{i=1}^{n_{cb}}\sum_{j=1}^{n_{cb}}(y_j)^2(G_c)_{ij}+\rho_k\sum_{k=1}^{n_b}(y_k)^2(G_s)_k-\rho_k\sum_{k=1}^{n_b}(y_k)^2(G_c)_k\right]\Delta A_c+\left[\rho_p\sum_{p=1}^{n_{st}}(y_p)^2(G_{st})_p-\rho_p\sum_{p=1}^{n_{st}}(y_p)^2(G_c)_p\right]\Delta A_c \tag{25}$$

$$ES_y=\left[\sum_{i=1}^{n_{cb}}\sum_{j=1}^{n_{cb}}(z_j)(G_c)_{ij}+\rho_k\sum_{k=1}^{n_b}(z_k)(G_s)_k-\rho_k\sum_{k=1}^{n_b}(z_k)(G_c)_k\right]\Delta A_c+\left[\rho_p\sum_{p=1}^{n_{st}}(Z_p)(G_{st})_p-\rho_p\sum_{p=1}^{n_{st}}(Z_p)(G_c)_p\right]\Delta A_c \tag{26}$$

$$ES_z=\left[\sum_{i=1}^{n_{cb}}\sum_{j=1}^{n_{cb}}(y_j)(G_c)_{ij}+\rho_k\sum_{k=1}^{n_b}(y_k)(G_s)_k-\rho_k\sum_{k=1}^{n_b}(y_k)(G_c)_k\right]\Delta A_c+\left[\rho_p\sum_{p=1}^{n_{st}}(y_p)(G_{st})_p-\rho_p\sum_{p=1}^{n_{st}}(y_p)(G_c)_p\right]\Delta A_c \tag{27}$$

$$EI_{zy}=\left[\sum_{i=1}^{n_{cb}}\sum_{j=1}^{n_{cb}}(y_j)(z_j)(G_c)_{ij}+\rho_k\sum_{k=1}^{n_b}(y_k)(z_k)(G_s)_k-\rho_k\sum_{k=1}^{n_b}(y_k)(z_k)(G_c)_k\right]\Delta A_c$$
$$+\left[\rho_p\sum_{p=1}^{n_{st}}(y_pZ_P)(G_{st})_p-\rho_p\sum_{p=1}^{n_{st}}(y_pZ_P)\ (G_c)_p\right]\Delta A_c \tag{28}$$

❖ STIFFNESS MATRIX

The sequence of derivation of the stiffness matrix starting from the principal of virtual displacements used by Yang and Mc Graw (1986) was applied herein. However, they analyzed thin-walled axi-symmetric steel sections, ie. pure steel beam columns. Hence, they included geometric nonlinearity only. In the present study a new stiffness matrix considering both geometric and material nonlinearities is deduced. The matrix takes into account the inclination of neutral axis concrete crack diffusion, and steel yielding at increasing load levels. The details of the formulation are given by Zaki (2001). The system of equations of equilibrium thus will be in the form

$$[k]\{u\}=\{f\} \tag{29}$$

where [k] is the total of the elastic and geometric stiffness matrices of the column segment given in the Appendix, {u} is the nodal displacement vector and {f} is the nodal force vector.

The segment stiffness matrices are assembled through an updated transformation matrix.

❖ VERIFICATION OF THE METHOD

The method of solution and program were verified against the column presented by Saadatmanesh, Ehsani and Li (1994). The comparison is shown in Figure 8.

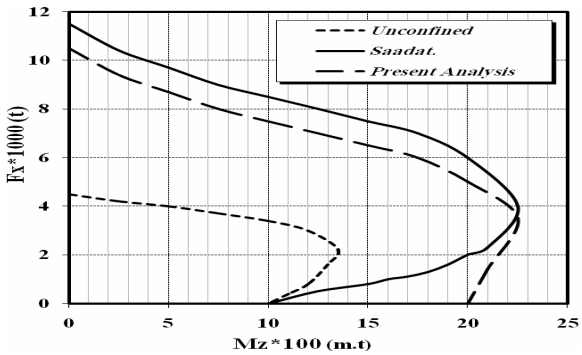

Figure 8. Curves for Saadatmanesh, Ehsani& Lie and present analysis

The column is a prototype bridge column of diameter 1.524 m, 32 steel reinforcing bars were used for the longitudinal reinforcement to give a total steel area equal 46.464 mm^2. The concrete used is of 3000 t/m^2 compressive strength. Carbon straps of thickness 5 mm covered the whole length of the column. The properties of steel and carbon straps are as given in the section introducing the stress-strain diagram. The interaction diagrams show plots of the predefined column in addition to a plot of a column having the same section without straps.

The unstrapped column, the interaction diagram of the present analysis nearly coincides with that of Saadatmanesh, Ehsani and Li. For the confined column the present analysis gives nearly 10% decrease in the ultimate axial load. Both curves go in accordance except for the region where the moment is dominant. The present analysis declares that retrofitting of the column remarkably increases the capacity of the beam-column in bending.

❖ CONTOURS OF PRESENT ANALYSIS

The present study is conducted for a circular column of diameter 50 cm, concrete grade 3000 t/m2. The longitudinal bars are 10 bars of total area 20.1cm2. Four cross-sections are considered, the first section includes the FRP as an imbedded I-beam section. The I-beam has the dimension 22*1.5 cm upper and lower flange, and 20*1.5 cm web. The concrete in this case is considered unconfined and denoted as I. The second section is strapped using six carbon straps each of thickness 10 mm. The strap width s and the clear spacing between straps s' are equal. The case is denoted as P which study for partially confined. The third column is fully confined along its length using 5 mm strap thickness. This case is denoted as F which stands for fully confined. A fourth column having the same section and with no FRP is used as a reference and is denoted by R. All columns are pin-ended at both ends, subjected to an axial force together with equal and opposite end moments at the ends. Each of the four columns is studied for three slenderness ratios; l/r=0, l/r=50 and l/r=100. Table 1 shows the notations for the different columns.

Table 1. Properties of each I model Confined Strapped. For steel grade 52, Concrete Strength (fcu)=300 Kg/cm2, and the same volume of FRP

Slenderness (l/r)	Strapped	case
0.0	I1	I beam imbedded
50.0	I2	
100.0	I3	
0.0	P1	Partially confined
50.0	P2	
100.0	P3	
0.0	F1	Fully confined
50.0	F2	
100.0	F3	
0.0	R1	Reference
50.0	R2	
100.0	R3	

I= imbedded FRP in the column as I section
P= 50% of column length is covered by FRP straps
F=The column is totally covered by FRP straps
R= Reference column

All models are subjected to an axial compression force with equal and opposite end moments about each of the y-axis and z-axis. Contour lines are plotted. The nondimensional variable for axial load F_x is given as:

$$P = \frac{F_x}{F_{xu}} \qquad (30)$$

where F_{xu} is the squash load.

Figure 9 demonstrates an increase in the squash load F_{xu} equal to 63%, 70% and 139% in the case of L/r=0 for models I, P and F respectively over the reference model R. However these percentages decrease with increasing the slenderness ratio l/r. For l/r=50, the recorded increase in F_{xu} is 49%, 52%, 91% while for l/r=100 the increase is 17%, 22% and 27% for models I, P and F respectively.

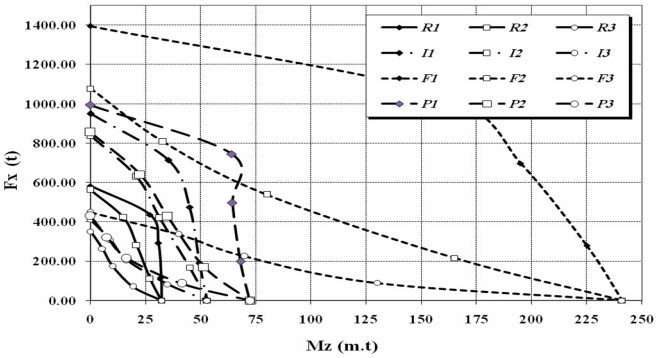

Figure 9. Interaction Diagrams for all Mod

The results show that the increase in the axial load of the fully confined columns, Model F, is greatly remarkable over model I reaching a difference 69% while this difference decrease as l/r increases reaching only 10% in case of l/r=100. It is also noted that results of model P are closer to model I than model F.

The same curve, Figure 9, show that the increase gained in the bending moments is 64%, 122% and 643% for models I, P and F respectively.

Figures (10 to 21) are contour lines plotted between M_z and M_y at different nondimensional axial loads p=0.0, 0.2, 0.5, and 0.75. Figures 10, 11 and 12 are plotted for model I at l/r=0.0, 50 and 100

respectively. Figs (13 to 15), Figs (16 to 18) and Figs (19 to 21) are corresponding plots for models P, F and R respectively. Generally, it is observed that a dip occurs at M_z nearly half of its ultimate value M_{zu}

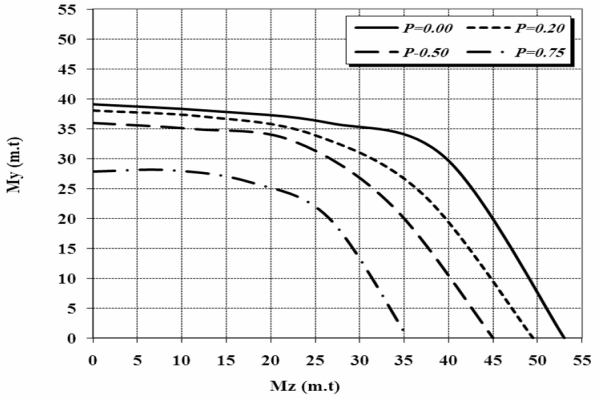

Figure 10. Contour Lines for Model I, l/r=0

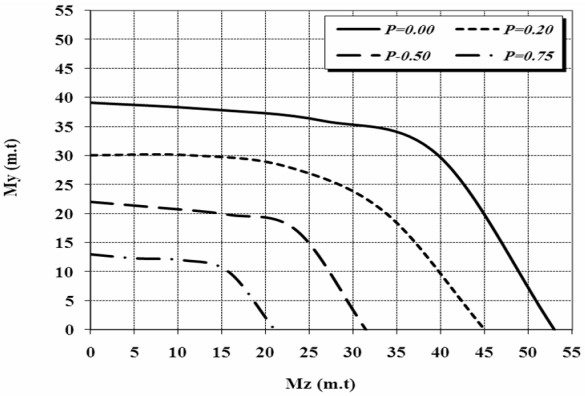

Figure 11. Contour Lines for Model I, l/r=50

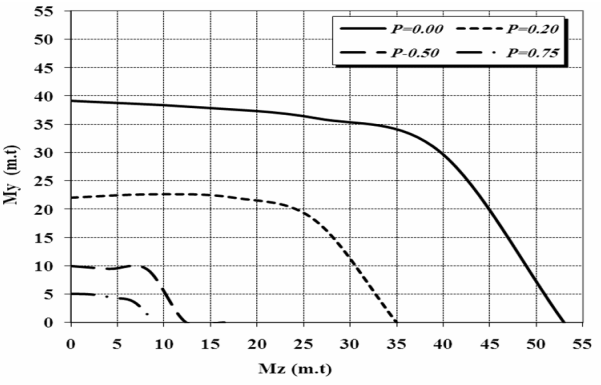

Figure 12. Contour Lines for Model I, l/r=100

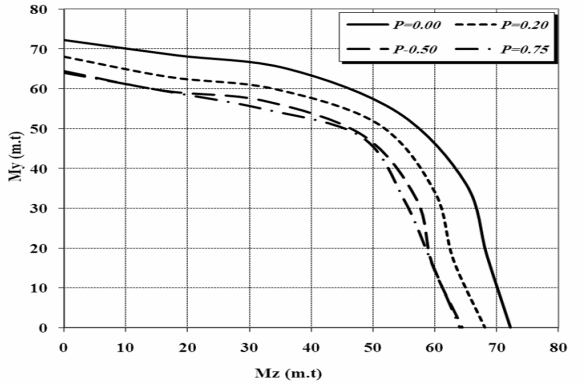

Figure 13. Contour Lines for Model P, l/r=0

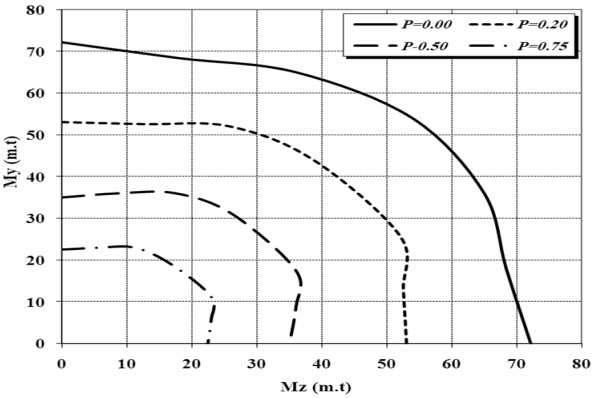

Figure 14. Contour Lines for Model P, l/r=50

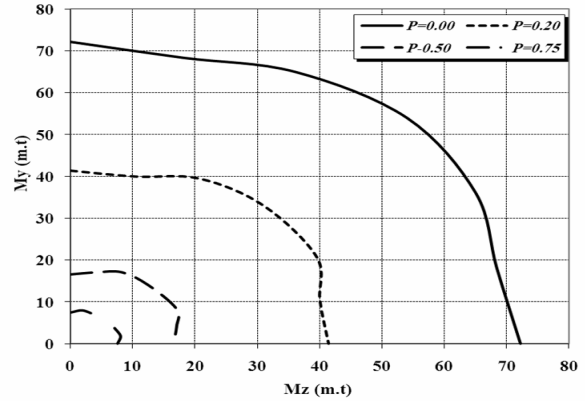

Figure 15. Contour Lines for Model P, l/r=100

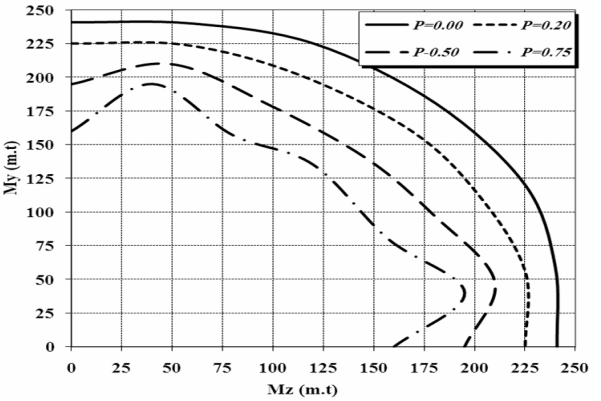

Figure 16. Contour Lines for Model F, l/r=0

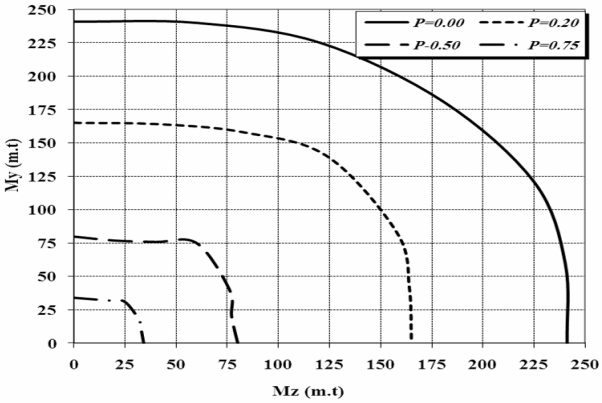

Figure 17. Contour Lines for Model F, l/r=50

The curves in the cases P, F and R do not show symmetry about the 45 degree radial line. This is due to the way of loading. The axial load together with the moment about the z-axis were increased simultaneously till the desired values, then increments of the moments M_y were introduced to the column till failure. As an example loading the column to 0.75 M_{zu} leads to failure at M_y much lesser than loading it to 0.25 M_{zu}.

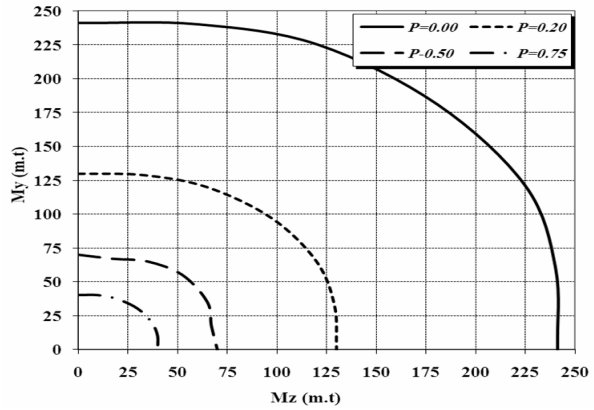

Figure 18. Contour Lines for Model F, l/r=100

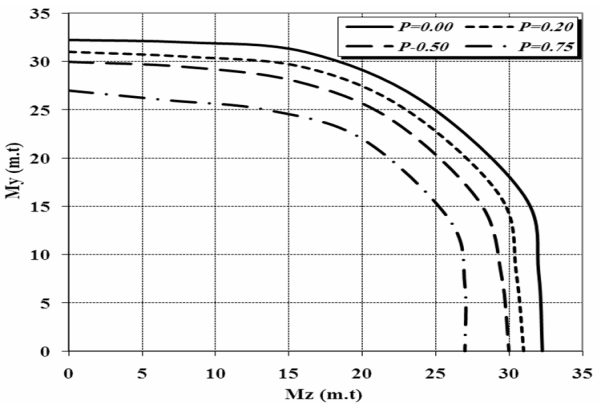

Figure 19. Contour Lines for Model R, l/r=0

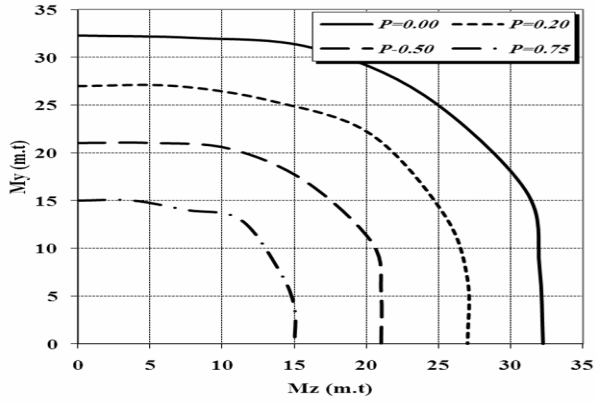

Figure 20. Contour Lines for Model R, l/r=50

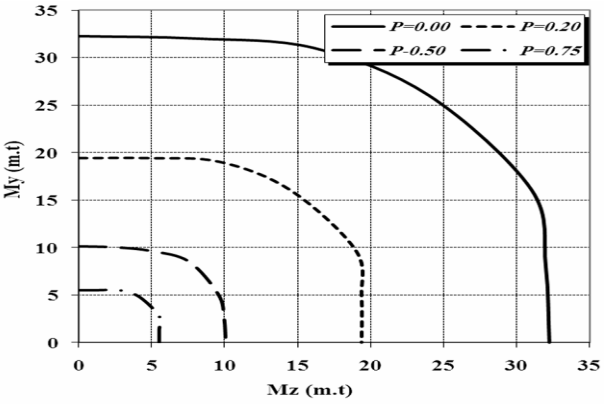

Figure 21. Contour Lines for Model R, l/r=100

The curves indicate that as p increases a less increase of the ultimate moment is achieved. Taking case I, l/r=0.0 as an example, the bending moment about the Z-axis achieves an increase of 65%, 53%, 50% and 30% over the reference R model in case of p=0.0, 0.20, 0.50 and 0.75 respectively. The increase in the maximum moment capacity is less in case of l/r=50 and much less in case of l/r=100. This is remarkable in the P and F models. However, in the case of I model slight discrepancies of the moment capacity are observed by changing the slenderness ratio.

It is conducted that the use of FRP as external confinement all over the length of the column give remarkable increase in strength results beyond partial confining although the thickness of FRP straps and doubled to achieve the same volume of FRP used. Using the same volume of FRP as imbedded reinforcement give less increase in strength capacity compared with external confining.

❖ CONCLUSIONS

A reliable analytical solution of the problem of circular biaxial composite columns with different slenderness ratios is now available. The designer could be easily directed to choose the method of utilizing FRP to solve the beam-column under the applied loads and given length.

The problem was solved for pin-ended columns with loads applied at the ends. However, the problem can be solved for any case of loading and end-conditions of the columns.

❖ NOTATIONS

The following symbols are used in this paper

A=Area.
b=Diameter of concrete section.
E=Modulus of elasticity.
e_y, e_z= *Eccentricities of normal force about y-axis and z-axis respectively*
F=Force.
$b^{\parallel}$= *Diameter of the circle at which the longitudinal bars are spaced.*
F_{xu}=*Squash load.*
f=Stress.
{f}=Force vector.
G= Elemental modulus of elasticity.
I=Inertia.
k_1=*Strength reduction factor for concrete.*
M=Moment.
m=Nondimentional axial force moment.
N.A.=Neutral axis
n=Number of element in concrete section.
p =Nondimentional axial force.
Q=Imaginary origin outside the section.
{u}=Segment displacement vector.
Z=Perpendicular distance from the centroid of each element of the cross-section to the neutral axis.
Z_n=*Perpendicular distance from the corner of maximum strain to the neutral axis.*
ε=*Normal strain.*
Ψ=*Inclination of the vector* Φ *to the z-axis.*
Φ=*Curvature.*
ρ =*Element material area to elemental concrete area.*
ΔA=*Elemental area.*
n_{cb}=*Number of rows or columns of elemental concrete areas.*

Subscripts

c=Concrete.
e=Elastic.
y=Yield of steel.
x,y,z=Coordinates.
i,j=Counters to determine elemental concrete area.
k=Counters to determine steel bar.
p=Counters to determine FRP elemental area.

❖ REFERENCES

[1.] Rousakis T. C., Karabins A. I., Kousis P.D. and Tepfers R. "Analytical Model of plastic Behavior of Uniformly FRP Confined Members", Composites Part B: Engineering, Vol. 39, Issues 7-8, October-December 2008, pp 1104-1113.

[2.] Harajli M. H. "Axial Stress-Strain Relationship for FRP Confined Circular and Rectangular Concrete Columns" Cement and Concrete Composites, Vol. 28, Issue 10, Nov. (2006), pp 938-948.

[3.] Binici B., "Design of FRPs in Circular Bridge Column Retrofits for Ductility Enhancement" Engineering Structures, Vol. 30, Issue 3, March. 2008, pp. 766-776.

[4.] Harajli M. H. "Bond Strengthening of Lap Spliced Reinforcement Using External FRP Jackets: An Effective Technique for Seismic Retrofit of Rectangular or Circular RC Columns", Construction and Building Materials, Vol. 23, Issue 3, March 2009, pp 1265-1278.

[5.] Lam L. and Teng J. G., "Stress-Strain Model for FRP Confined Concrete Under Cyclic Axial Compression" Engineering Structures, Vol. 31, Issue 2, Feb. 2009, pp 308-321.

[6.] Tastani S. P. and Pantazopoulou S.J., "Detailing Procedures for Seismic Rehabilitation of Reinforced Polymers", Engineering Structures, Vol. 30, Issue 2, Feb. 2008, pp 450-461.

[7.] Cheng H.L., Solelino E. D., and Chen W. F., "Sensitivity Study and Design Procedure for FRP Wrapped Reinforced Concrete Circular Columns" International Journal of Applied Science and Engineering Vol. 2 Issue 2 June 2004, pp 148-162.

[8.] Tavarez F. A., Bank L. C., and Plesha M.E., "Analysis of Fiber-Reinforced Polymer Composite Grid Reinforced Concrete Beams", ACI, Structural Journal, Vol. 100 No. 2, March-April 2003, pp 250-258.

[9.] Issa M. A., Alrousan R. Z., and Issa M.A., "Experimental and Parametric Study of circular Short Columns Confined With CFRP Composites", ASCE, J. Comps, for Constr., Vol. 13, Issue 2, March-April 2009, pp 135-147.

[10.] Popovics S., "Numerical Approach to the Composite Stress-Strain Curves for Concrete", Cement of Concrete Research, Vol. 3, No. 5, 1973, pp. 583-599.

[11.] Saadatmanesh, H., Ehsani, M. R., and M.W. Li, "Strength and Ductility of Concrete Columns externally Reinforced with Fiber Composite Straps" ACI Structural Journal, Vol. 91, No. 4 July-August 1994, pp. 434-447.

[12.] Scott B. D., Park R. and Priestley M. T. N., "Stress-Strain Behavior of Concrete Confined by Overlapping Hoops at Low and Hight Strain Rates" ACI Journal, Proceedings Vol. 79, No. 1 Jan-Feb. 1982, pp. 13-27.

[13.] Yang Y.B., and McGraw W., "Stiffness Matrix For Geometric Nonlinear Analysis", Journal of Structural engineering, ASCE Vol. 112, April 1986, pp. 853-877.

[14.] Zaki M. K., "Design of Composite Beam-Columns Under Bending" ph.D. Faculty of Engineering, Cairo University, Giza, Egypt, May 2001.

[15.] Mander J.B., Priestley M.J.N., and Park R.," Theoretical Stress-Strain Model for Confined Concrete" Journal of Structural engineering, ASCE Vol. 114, No. 8, Aug 1988, pp. 1804-1826.

ANNALS OF FACULTY ENGINEERING HUNEDOARA
– INTERNATIONAL JOURNAL OF ENGINEERING